Self-Assembly

DOI: 10.1002/anie.200904566

Highly Stable Pleated-Sheet Secondary Structure in Assemblies of Amphiphilic α/β-Peptides at the Air–Water Interface**

Shlomit Segman, Myung-ryul Lee, Vladimir Vaiser, Samuel H. Gellman, and Hanna Rapaport**

There is growing interest in the design of molecules that undergo predictable self-assembly. Such systems offer the prospect of tuning the properties of materials based on precise tailoring of molecular structure. Progress in this field is driven both by fundamental scientific curiosity and by the numerous potential applications that can be envisioned for "smart" materials. Peptides are attractive as building blocks for self-assembling materials because it is easy to incorporate a wide array of functionality onto the side chain of these molecules because peptides tend to be biocompatible, and the rules that govern peptide self-association are moderately well understood.[1] Bioinspired oligomers with well-defined conformational propensities, called "foldamers",[2] have comparable advantages for materials applications,[3] and they resist proteolytic degradation.[4] Herein we describe designed amphiphilic oligomers that contain both α-amino acid and β-amino acid residues, which are called "α/β-peptides". These amphiphilic oligomers are intended to assemble through the formation of hydrogen-bonded sheets at the air–water interface.

The two α/β-peptides we examined, **βKβE** and **βEβK**, differ in the positions of the ionizable side chains, which are provided by β^3-homolysine (β^3hLys) and β^3-homoglutamic acid (β^3hGlu) residues, and both contain 11 residues with 1:1 alternation of α and β subunits along the backbone.

βKβE Ac-Pro-β^3hPhe-Val-β^3hLys-Thr-β^3hPhe-Val-β^3hGlu-Thr-β^3hPhe-Pro-NH_2

βEβK Ac-Pro-β^3hPhe-Val-β^3hGlu-Thr-β^3hPhe-Val-β^3hLys-Thr-β^3hPhe-Pro-NH_2

[*] M. R. Lee, Prof. Dr. S. H. Gellman
Department of Chemistry, University of Wisconsin
1101 University Avenue, Madison, WI 53706 (USA)
E-mail: gellman@chem.wisc.edu
S. Segman, V. Vaiser, Dr. H. Rapaport
Department of Biotechnology Engineering
Ben Gurion University of the Negev
PO Box 653, Beer-Sheva 84105 (Israel)
Fax: (+972) 8-6472983
E-mail: hannarap@bgu.ac.il

[**] This work was supported by the United States–Israel Binational Science Foundation (Grant No. 2005132). M.-r.L. was supported by a Korea Research Foundation Grant funded by the Korean Government (MOEHRD) (KRF-2006-214-C00053) and by the Nanoscale Science and Engineering Center at UW-Madison (NSF DMR-0425880). GIXD studies at beam-line BW1, Hasylab, DESY, were supported by the European Community-Research Infrastructure Action under the FP6 "Structuring the European Research Area" Programme (through the Integrated Infrastructure Initiative "Integrating Activity on Synchrotron and Free Electron Laser Science").

Supporting information for this article is available on the WWW under http://dx.doi.org/10.1002/anie.200904566.

In an extended conformation, this α/β-peptide backbone can engage in interstrand H-bonding analogous to that found in β-sheets formed by α-peptide strands, as illustrated below.[2]

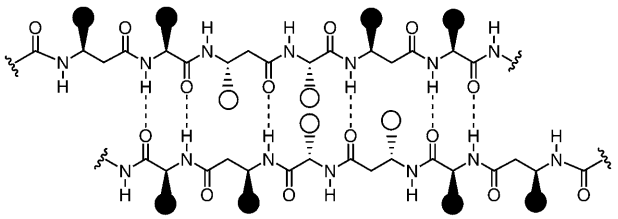

Small capping groups are placed at each N- and C-terminus to prevent development of a charge at these positions.[3] The residues at the terminal are derived from proline, which is intended to promote alignment of α/β-peptide molecules along the H-bond direction within two-dimensional sheet assemblies.[4] All of the α-residues (Val and Thr) have a branched side chain. This design feature is based on our previous observation that such α-residues strongly destabilize helical secondary structure among α/β-peptides that have a 1:1 α/β pattern, and which should encourage the desired extended conformations.[5] The α/β-peptide sequences are defined by an alternating pattern of hydrophobic dyads (β^3hPhe-αVal) and hydrophilic dyads (β^3hLys-αThr or β^3hGlu-αThr). As indicated in the structure above this sequence pattern causes the hydrophobic side chains to project from one side of the extended α/β backbone and the hydrophilic side chains to project from the other side, thus giving rise to global amphiphilicity. This prediction is based on the assumption that the β-residues adopt conformations with backbone θ torsion angles [NC–CC(=O)] of approximately 180°, as has generally been observed for β-residues in sheet secondary structures.[6] The intended clustering of hydrophobic and hydrophilic side chains on opposite sides of the backbone is expected to promote sheet assembly at the air–water interface, as the hydrophilic side chains can project into the aqueous phase while the hydrophobic side chains project into the air. Notably, the sequential arrangement of hydrophobic and hydrophilic side chains that gives rise to global amphiphilicity in an extended conformation is quite different for these α/β-peptides relative to conventional α-peptides; in the latter case, hydrophobic and hydrophilic side chains are arranged in a 1:1 alternating pattern.

Previously, we have utilized Langmuir films at the air–water interface to direct the assembly of designed amphiphilic α-peptides into two-dimensionally ordered β-sheet monolayers.[7] Our design approach and the experimental evaluation

of the peptides by characterization of two-dimensional crystalline films formed by these molecules, provide a powerful tool for establishing relationships between α-amino acid sequence and assembly behavior.[7,8] The insights that emerge from these fundamental studies provide a basis for subsequent designs that are intended to achieve functional goals. Thus, for example, amphiphilic β-sheet-forming α-peptides have been utilized as templates for biomineralization,[9,10] in patterning of nanoparticles,[11] and in the formation of hydrogels.[12] These precedents inspired our design of the amphiphilic α/β-peptides described below.

Grazing incidence X-ray diffraction (GIXD) measurements at the air–water interface may provide direct structural information at the sub-nanometer scale on Langmuir crystalline monolayers.[13] The GIXD patterns of the **βKβE** and **βEβK** monolayers revealed large differences (Figure 1 and

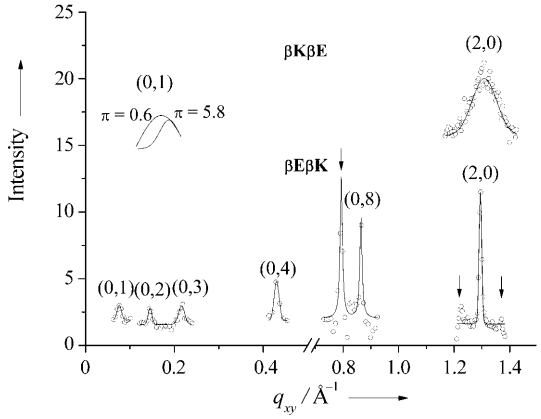

Figure 1. GIXD intensity versus q_{xy} patterns of **βKβE** (top) and **βEβK** (bottom) on deionized water at $\pi = 9$ mN m^{-1}. Intensities in the region of the $q_{xy} \approx 1.3$ Å^{-1} Bragg peak divided by five. Bragg peaks marked by arrows were assigned to a subunit cell (see text). Experimental points were fitted with Gaussian curves except for the relatively weak Bragg peaks on both sides of $q_{xy} \approx 1.3$ Å^{-1}. Experimental points in **βKβE** (0,1) Bragg peak were omitted to clearly show the shift in peak maxima following the increase in surface pressure.

Table 1S in the Supporting Information). At low surface pressure, $\pi = 0.6$ mN m^{-1}, **βKβE** exhibited two Bragg peaks at $q_{xy} = 0.1523$ and 1.3085 Å^{-1} that correspond to spacing 41.3 Å along the long axis of the oligomer and spacing 4.80 Å along the hydrogen bond direction, which are indexed (0,1) and (2,0), respectively, in two-dimensional ordered assemblies. The (0,1) Bragg peak shifted to 33.1 Å with an increase in surface pressure to $\pi = 5.8$ mN m^{-1} (Figure 1 top and Table 1S in the Supporting Information), thus demonstrating that these crystalline assemblies are compressible along the long axis spacing of the oligomer.[14] The full width at half maxima (FWHM) of the Bragg peaks correlates with the extent of order, that is, coherence length in the domain (Table 1S in the Supporting Information) hence, the number of molecules that contribute to the order may be estimated by dividing the coherence length of a Bragg peak by its spacing. The rather wide Bragg peaks of **βKβE** indicate that only about 9–14 strands are ordered along the (2,0) H-bond direction and only 3–6 strands along the (1,0) direction. In contrast, **βEβK** exhibited a diffraction pattern with nine sharp Bragg peaks that appear at $\pi = 9$ mN m^{-1} (Figure 1 bottom and Table 1S in the Supporting Information), thus indicating superiority in the extent of order compared to **βKβE** and to any previously studied β-sheet monolayers of α-peptides, which typically show only 2–4 Bragg peaks in GIXD.[15] In addition, the crystalline film formed by **βEβK** showed no shifts in the $(0,h)$ peak positions upon compression to $\pi = 16$ mN m^{-1}, thus giving assemblies that are highly stable and resistant to compression. The Bragg peaks observed at $\pi = 9$ mN m^{-1}, at $q_{xy} \approx 0.0751$, 1.448, 0.2166, 0.4301, and 0.8649 Å^{-1}, correspond to a $d_{(0,1)}$ spacing of about 83.7 Å and its higher order reflections (Figure 1 and Table 1S in the Supporting Information). The peak at $q_{xy} = 1.2946$ Å^{-1}, $d = 4.85$ Å most probably defines the spacing along the interstrand H-bond direction. Based on these data, the unit cell formed by **βEβK** is $a =$ 9.7 Å, $b \approx 86.8$ Å, $\gamma \approx 90°$. The b axis was determined more accurately, owing to the rather weak intensity of the peak at $q_{xy} \approx 0.0751$ Å^{-1}, as double the $d_{(0,2)} = 43.4$ Å spacing. The a axis is twice the 4.85 Å spacing, which can be accommodated by an antiparallel arrangement of neighboring strands (Figure 2). The three peaks observed at $q_{xy} = 0.7921$, ≈ 1.220, and ≈ 1.365 Å could not be associated with the main unit cell; these peaks could be attributed to a subunit cell generated by the repeat structural motif of the oligomer dyads, which is described below along with a proposed molecular model.

We hypothesize that the higher stability exhibited by **βEβK** compared to **βKβE** arises from differences in the ways that the charged side chains interact with the molecular dipole of the α/β-peptide backbone in the pleated strand conformation. An α-peptide in a β-strand conformation has a small net dipole—positive at the N-terminus and negative at the C-terminus, because the carbonyl groups are slightly tilted relative to the normal to the backbone vector, with the carbonyl oxygen atom pointing toward the C-terminus.[16] The net dipole moment of a β-strand has a direction relative to the backbone (+N→C−) which is similar to that of an α-helix, but the latter has a much larger net dipole because the carbonyl groups are nearly aligned with the axis of the helix. In **βKβE**, the cationic β^{3}hLys is close to the N-terminus and the anionic β^{3}hGlu is close to the C-terminus; these positions are reversed in **βEβK**. If the α/β-peptide backbone in the strand conformation has a net dipole analogous to that of an α-peptide in the strand conformation, then the charged side chains in **βKβE** should interact unfavorably with the backbone dipole, while the charged side chains in **βEβK** should interact favorably with this dipole. Thus, the strand conformation of **βEβK** should be more stable than the strand conformation of isomeric **βKβE**, and this could lead to the difference we observe in the stability of the assemblies formed by these two α/β-peptides.

We constructed a model of the crystalline assembly formed by **βEβK** at the air–water interface based on the repeat distances obtained from the diffraction data and simple conformational assumptions. This model was generated by extrapolation from structural features of β-sheets formed by α-peptides. We assumed that the backbone of the α/β-peptide adopts a pleated conformation that allows the

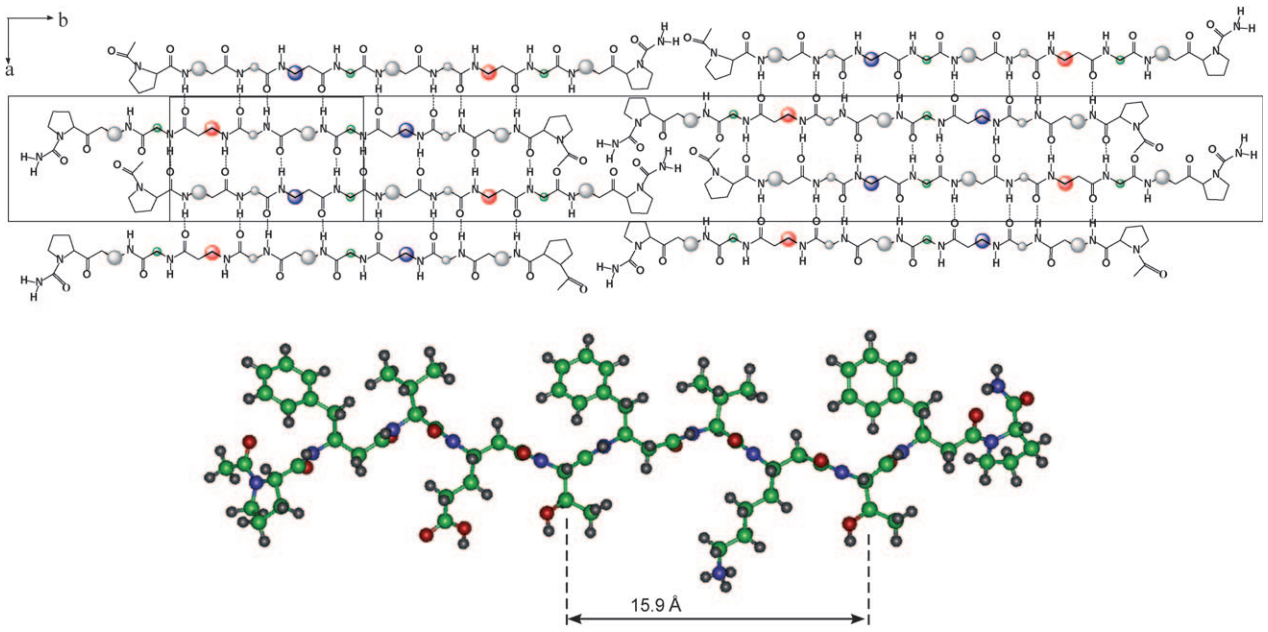

Figure 2. Proposed two-dimensional lattice of the amphiphilic oligomer **βEβK** packed in antiparallel mode. Circles denote side chains of amino acids, hydrophobic amino acids, βPhe (large gray circles) and Val (small gray circles), hydrophilic amino acids βLys (blue), Thr (green), and βGlu (red) circles, respectively). The large rectangle represents the unit cell $a = 9.7$, $b \approx 86.8$ Å, $\gamma \approx 90°$ and the small one represents a subunit cell $a_s = 9.7$, $b_s = 15.9$ Å, $\gamma \approx 90°$ generated by the pleated structure of the oligomer (shown at the bottom in a ball and stick representation with carbon (green), oxygen (red), amine (blue), and hydrogen (gray), respectively).

hydrophobic side chains, from β^3hPhe and Val, to project from one face of the sheet, while the hydrophilic side chains, from β^3hGlu, β^3hLys, and Thr, project from the other face. Neighboring strands were arranged in an antiparallel fashion and are positioned so as to maximize the number of interstrand H-bonds (Figure 2). The best arrangement was obtained for neighboring strands with about 7.9 Å offset along the *b* direction, which allowed almost all interstrand C=O···H–N H-bonds to form (Figure 2). In this model the α residues were positioned to form interstrand H-bond patterns similar to those in a conventional antiparallel β-sheet. The β residues were then adjusted to form interstrand H-bonds while pointing their side chains to the appropriate side of the sheet. This molecular model exhibits a unique pleated structure that was found to accommodate both the main unit cell and the repeat distances that we assumed to belong to a subunit cell in the lattice.

The subunit cell was necessary to explain the three Bragg peaks observed for **βEβK** (peaks are denoted by arrows in Figure 1 and Table 1S in the Supporting Information, $\pi = 9$) at $q_{xy} = 0.7921$, ≈ 1.220, and ≈ 1.365 Å, corresponding to 7.93, ≈ 4.60, and ≈ 5.16 Å spacings. Based on the repeat distance of ≈ 7.9 Å, which matches the projected length of every two amino acid in the model, a subunit cell $a_s = 9.7$, $b_s = 15.9$ Å was constructed that allowed indexing the 7.93, 5.16, and 4.6 Å repeat distances $(0,2)_s$, $(0,3)_s$, and $(1,3)_s$, respectively. The subunit cell b_s axis spans the intrastrand length of every four residues (α-β-α-β), composing the repeat motif of the sheet, as for example the Thr–Thr distance (Figure 2). This $(0,2)_s$ Bragg peak, at $q_{xy} = 0.7921$ Å, exhibits a relatively strong intensity indicative of the abundance of this quasi-twofold symmetry motif relating the hydrophobic and hydrophilic dyads, which point to opposite faces of the sheet. The rather weak intensities observed for the $(0,3)_s$ and $(1,3)_s$, at $q_{xy} = 1.220$ and 1.365 Å may be rationalized by the lack of threefold symmetry within the subunit cell.

We have reported the de novo design and characterization of amphiphilic α/β-peptides that form ordered two-dimensional assemblies at the air–water interface. Our results show that positioning of ionic side chains along the backbone can exert a profound effect on the propensity to self-assemble, presumably because of intramolecular backbone dipole-charge interactions. These assemblies exhibit structural similarities to those of β-sheet-forming α-peptides, but the α/β-peptide assemblies can display stability that is unparalleled among α-peptide assemblies. This high stability leads to an unusually rich GIXD data set, which has allowed us to construct a detailed model of an antiparallel α/β-peptide sheet structure that reveals a unique pleated structure of the α/β-peptides. Further studies should provide a clearer understanding of the origin of the remarkable structural stability available to amphiphilic α/β-peptide sheets.

Received: August 16, 2009
Published online: December 17, 2009

Keywords: β-sheet · foldamers · monolayers · peptides · self-assembly

[1] a) E. T. Powers, S. I. Yang, C. M. Lieber, J. W. Kelly, *Angew. Chem.* **2002**, *114*, 135–138; *Angew. Chem. Int. Ed.* **2002**, *41*, 127–130; b) S. Zhang, *Nat. Biotechnol.* **2003**, *21*, 1171–1178; c) A. Aggeli, M. Bell, L. M. Carrick, C. W. Fishwick, R. Harding, P. J. Mawer, S. E. Radford, A. E. Strong, N. A. Boden, *J. Am. Chem.*

Soc. **2003**, *125*, 9619 – 9628; d) J. K. Kretsinger, L. A. Haines, B. Ozbas, D. J. Pochan, J. P. Schneider, *Biomaterials* **2005**, *26*, 5177 – 5186.

[2] a) S. H. Gellman, *Acc. Chem. Res.* **1998**, *31*, 173 – 180; b) R. P. Cheng, S. H. Gellman, W. F. DeGrado, *Chem. Rev.* **2001**, *101*, 3219 – 3232; c) *Foldamers: Structure, Properties, and Applications* (Eds.: S. Hecht, H. Ivan), Wiley-VCH, Weinheim, **2007**; d) C. M. Goodman, S. Choi, S. Shandler, W. DeGrado, *Nat. Chem. Biol.* **2007**, *3*, 252 – 262; e) W. S. Horne, S. H. Gellman, *Acc. Chem. Res.* **2008**, *41*, 1399 – 1408.

[3] a) W. C. Pomerantz, N. L. Abbott, S. H. Gellman, *J. Am. Chem. Soc.* **2006**, *128*, 8730 – 8731; b) T. A. Martinek, A. Hetenyi, L. Fulop, I. M. Mandity, G. K. Toth, I. Dekany, F. Fulop, *Angew. Chem.* **2006**, *118*, 2456 – 2460; *Angew. Chem. Int. Ed.* **2006**, *45*, 2396 – 2400; c) R. W. Sinkeldam, F. J. M. Hoeben, M. J. Pouderoijen, I. De Cat, J. Zhang, S. Furukawa, S. De Feyter, J. A. J. M. Vekermans, E. W Meijer, *J. Am. Chem. Soc.* **2006**, *128*, 16113 – 16121; d) W. C. Pomerantz, K. D. Cadwell, Y.-J. Hsu, S. H. Gellman, N. L. Abbott, *Chem. Mater.* **2007**, *19*, 4436 – 4441; e) W. C. Pomerantz, V. M. Yuwono, C. L. Pizzey, J. D. Hartgerink, N. L. Abbott, S. H. Gellman, *Angew. Chem.* **2008**, *120*, 1261 – 1264; *Angew. Chem. Int. Ed.* **2008**, *47*, 1241 – 1244; f) C. L. Pizzey, W. C. Pomerantz, B.-J. Sung, V. M. Yuwono, J. D. Hartgerink, S. H. Gellman, A. Yethiraj, N. L. Abbott, *J. Chem. Phys.* **2008**, *129*, 095103/1 – 095103/8.

[4] D. Seebach, A. K. Beck, D. J. Bierbaum, *Chem. Biodiversity* **2004**, *1*, 111 – 1239.

[5] M. A. Schmitt, S. H. Choi, I. A. Guzei, S. H. Gellman, *J. Am. Chem. Soc.* **2005**, *127*, 13130 – 13131.

[6] a) S. Krauthäuser, L. A. Christianson, D. R. Powell, S. H. Gellman, *J. Am. Chem. Soc.* **1997**, *119*, 11719 – 11720; b) Y. J. Chung, B. H. Huck, L. A. Christianson, H. E. Stanger, S. Krauthäuser, D. R. Powell, S. H. Gellman, *J. Am. Chem. Soc.* **2000**, *122*, 3995 – 4004; c) I. L. Karle, H. N. Gopi, P. Balaram, *Proc. Natl. Acad. Sci. USA* **2001**, *98*, 3716 – 3719.

[7] H. Rapaport, K. Kjaer, T. R. Jensen, L. Leiserowitz, D. A. Tirrell, *J. Am. Chem. Soc.* **2000**, *122*, 12523 – 12529.

[8] H. Rapaport, G. Möller, C. M. Knobler, T. R. Jensen, K. Kjaer, L. Leiserowitz, D. A. Tirrell, *J. Am. Chem. Soc.* **2002**, *124*, 9342 – 9343.

[9] S. Cavalli, D. C. Popescu, E. E. Tellers, M. R. J. Vos, B. P. Pichon, M. Overhand, H. Rapaport, N. A. J. M. Summerdijk, A. Kros, *Angew. Chem.* **2006**, *118*, 753 – 758; *Angew. Chem. Int. Ed.* **2006**, *45*, 739 – 744.

[10] S. Segman-Magidovich, H. Grisaru, T. Gitli, Y. Levi-Kalisman, H. Rapaport, *Adv. Mater.* **2008**, *20*, 2156 – 2161.

[11] H. Bekele, J. H. Fendler, J. W. Kelly, *J. Am. Chem. Soc.* **1999**, *121*, 7266 – 7267.

[12] H. Rapaport, H. Grisaru, T. Silberstein, *Adv. Funct. Mater.* **2008**, *18*, 2889 – 2896.

[13] H. Rapaport, I. Kuzmenko, M. Berfeld, R. Edgar, R. Popovits-Biro, I. Weissbuch, M. Lahav, L. Leiserowitz, *J. Phys. Chem. B* **2000**, *104*, 1399 – 1428.

[14] H. Isenberg, K. Kjaer, H. Rapaport, *J. Am. Chem. Soc.* **2006**, *128*, 12468 – 12472.

[15] H. Rapaport, *Supramol. Chem.* **2006**, *18*, 445 – 454.

[16] Y. K. Shin, M. D. Newton, S. S. Isied, *J. Am. Chem. Soc.* **2003**, *125*, 3722 – 3732.

